ISBN: 978-3-95450-253-0 ISSN: 2673-5571 doi:10.18429/JACoW-HB2023-THC1I2

FRIB BEAM POWER RAMP-UP: STATUS AND PLANS*

J. Wei†, C. Alleman, H. Ao, B. Arend, D. Barofsky, S. Beher, G. Bollen, N. Bultman, F. Casagrande, W. Chang, Y. Choi, S. Cogan, P. Cole, C. Compton, M. Cortesi, J. Curtin, K. Davidson, X. Du, K. Elliott, B. Ewert, A. Facco[1], A. Fila, K. Fukushima, V. Ganni, A. Ganshyn, T. Ginter, T. Glasmacher, J. Guo, Y. Hao, W. Hartung, N. Hasan, M. Hausmann, K. Holland, H. C. Hseuh, M. Ikegami, D. Jager, S. Jones, N. Joseph, T. Kanemura, S. H. Kim, C. Knowles, T. Konomi, B. Kortum, N. Kulkarni, E. Kwan, T. Lange, M. Larmann, T. Larter, K. Laturkar, R. E. Laxdal[2], J. LeTourneau, Z.-Y. Li, S. Lidia, G. Machicoane, C. Magsig, P. Manwiller, F. Marti, T. Maruta, E. Metzgar, S. Miller, Y. Momozaki[3], M. Mugerian, D. Morris, I. Nesterenko, C. Nguyen, P. Ostroumov, M. Patil, A. Plastun, L. Popielarski, M. Portillo, A. Powers, J. Priller, X. Rao, M. Reaume, S. Rogers, K. Saito, B. M. Sherrill, M. K. Smith, J. Song, M. Steiner, A. Stolz, O. Tarasov, B. Tousignant, R. Walker, X. Wang, J. Wenstrom, G. West, K. Witgen, M. Wright, T. Xu, Y. Yamazaki, T. Zhang, Q. Zhao, S. Zhao
Facility for Rare Isotope Beams, Michigan State University, East Lansing, MI, USA
P. Hurh, Fermi National Accelerator Laboratory, Batavia, IL, USA
S. Prestemon, T. Shen, Lawrence Berkeley National Laboratory, Berkeley, CA, USA
[1]also at INFN - Laboratori Nazionali di Legnaro, Legnaro (Padova), Italy
[2]also at TRIUMF, Vancouver, BC, Canada
[3]also at Argonne National Laboratory, Lemont, IL, USA

Abstract

This paper reports on the plans for a strategic ramp-up to high-beam-power operation of the Facility for Rare Isotope Beams, emphasizing challenges and solutions for beam-interception devices and targetry systems; radiation protection and controls; legacy systems renovation and integration; and automation and machine learning.

INTRODUCTION

The Facility for Rare Isotope Beam (FRIB) was completed in April 2022, ahead of the baseline schedule established about 10 years ago; the scientific user program started in May 2022 [1]. The ramp-up to the ultimate design beam power of 400 kW is planned over a six-year period (Fig. 1); 1 kW was delivered for initial user runs, and 5 kW was delivered as of February 2023. Primary beams delivered for rare isotope production include ^{36,40}Ar, ^{64}Zn, ^{48}Ca, ^{70}Zn, ^{82}Se, ^{86}Kr, ^{124}Xe, and ^{198}Pt. Test runs with 10 kW ^{36}Ar and ^{48}Ca beams were conducted in July 2023.

Extensive work has been done to prepare for high-power operation, including simultaneous acceleration of multiple charge states [2]; charge stripping of primary beams with liquid lithium [3]; commissioning of a superconducting electron-cyclotron-resonance ion source [4]; and operation of a rotating graphite target [5]. The superconducting radiofrequency (SRF) driver linac has been operating in continuous-wave (CW) mode as planned [6]. The linac setting is developed with a pulsed, low-average-power beam, while all experiments use a CW beam.

Although the driver linac is ready to deliver full-power beams, ramp-up of the average beam power requires facility-wide development. First, experience must be gained to safely handle increased radiological impact, including prompt radiation, activation in device materials and non-conventional utilities, and possible residual activation in ground water and exhaust air. Second, extensive machine studies and beam tuning are needed to minimize uncontrolled beam losses for the desired operating conditions. High-power targetry systems and beam-intercepting devices are in phased deployment along with ancillary systems, including non-conventional utilities and remote handling. Accelerator improvements and renovations to aging legacy systems are being implemented in parallel.

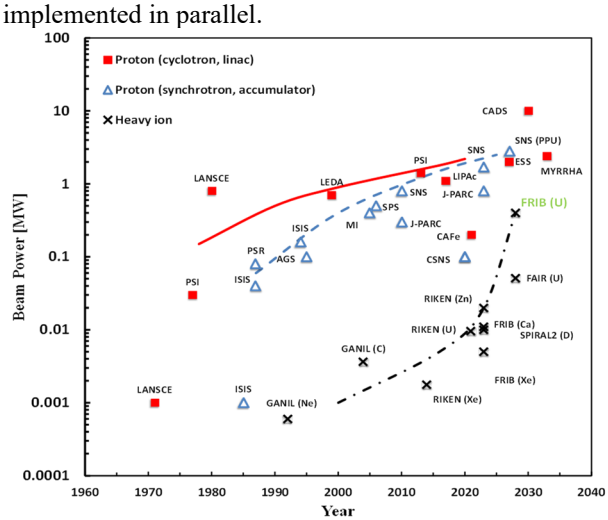

Figure 1: Beam power on target as a function of time for existing (as of August 2023) and planned power-frontier accelerator facilities.

* Work supported by the U.S. Department of Energy Office of Science under Cooperative Agreement DE-SC0023633, the State of Michigan, and Michigan State University.
† wei@frib.msu.edu

ISBN: 978-3-95450-253-0 ISSN: 2673-5571 doi:10.18429/JACoW-HB2023-THC1I2

PHASED LINAC IMPROVEMENTS

Linac improvements are planned for phased deployment to support operations and the power ramp-up, as shown in Table 1. Each "epoch" corresponds to about one year.

Table 1: Phased Driver Linac System Improvements (FS: Folding Segment; BDS: Beam Delivery System)

EPOCH	1	2	3	4	5	6
Beam Power	10 kW	20 kW	50 kW	100 kW	200 kW	400 kW
ARTEMIS, light ion beams from gas	■	■	■	■		
ARTEMIS, heavy ion beams from metal	■	■				
High Power ECR, gas beams	■	■	■	■	■	■
High Power ECR, metal beams	■	■	■	■	■	■
Intermediate power charge selector in FS1			■	■		
High power charge selector in FS1					■	■
Post-stripper chicane				■	■	■
Additional beam collimation in FS2, BDS				■	■	■
Dual charge state heavy ions upstream of the stripper (velocity equalizer)					■	■

Ion Sources

Both normal- (ARTEMIS) and super-conducting (SC) electron-cyclotron-resonance (ECR) ion sources are in operation, providing various species of primary beams needed for user experiments [4, 7]. In the first year of operations, a low temperature oven was used for lighter species (^{48}Ca, ^{70}Zn, ^{82}Se) and sputtering was used for heavier species (^{198}Pt, ^{238}U). A high-temperature inductive oven has been developed to routinely reach 1800-2000 ºC, facilitating higher-current Ni, Si and U beams. In parallel, a second SC ECR source is being designed for 28 GHz operation with a Nb_3Sn sextupole magnet [8]; thus 3 ECR sources will eventually be available to ensure high intensity with high operational availability.

Velocity Equalizer

The Low Energy Beam Transport (LEBT) was designed to transport dual-charge-state heavy-ion beams for 400 kW beams on target with a highly reliable mode of ECR operation. To produce a small longitudinal emittance, the dc beam from the ion source is bunched upstream of the radio-frequency quadrupole (RFQ) by an external multi-harmonic buncher (MHB) operating at 40.25, 80.5, and 120.75 MHz. The velocity of the dual-charge-state beam depends on the charge states; to minimize the effective longitudinal emittance, the velocities of each charge state beam must be equalized. A single-frequency 40.25 MHz resonator, a "velocity equalizer" (VE), will be installed between the MHB and RFQ for this purpose. The drift distance between the MHB and VE provides a 180° separation of the neighboring charge states. This drift space includes a biased tube with an adjustable voltage to ensure correct separation of different charge states for ion mass numbers above ~200. Two-charge-state acceleration upstream of the charge stripper and acceleration of up to 5 charge state downstream of the charge stripper help to maximize heavy-ion power delivery to the target.

Charge Stripper

The liquid lithium and rotating carbon charge strippers are installed adjacent to each other for operational flexibility [3]. The lithium stripper, designed to work with all beams at full power, has been successfully demonstrated with available beams, including uranium. At the current power level, there is no significant activation of materials in and around the strippers.

We have been gaining operational experience with lithium stripper performance. Instability observed in the film during extended runs was mitigated by maintenance cleaning. Efforts are being made to increase the film thickness for increased stripping efficiency, possibly by colliding two lithium jets in lieu of the current method with one jet impinging on a deflector. Trials with round water jets suggest that this approach is promising (Fig. 2).

Figure 2: Water film produced by colliding two jets from 1-mm diameter nozzles.

Charge Selector

The charge selector is designed to intercept the charge states of the stripped heavy ion beams that do not fit into the acceptance of the post-stripper linac segments. The existing charge selector, a pair of copper-alloy-based water-cooled jaws, is estimated to allow for beam delivery up to 50 kW. Upgraded versions for intermediate- and high-power operations are being designed. Figure 3 shows the intermediate-power design using two rotating graphite cylinders to intercept the unwanted charge states, distribute the beam-induced heating over a larger area, and radiate it to the water-cooled vacuum chamber walls. We expect the temperature of the graphite wheels to reach 2000 K, which will enhance annealing of the radiation damage and diffusion of implanted heavy ions.

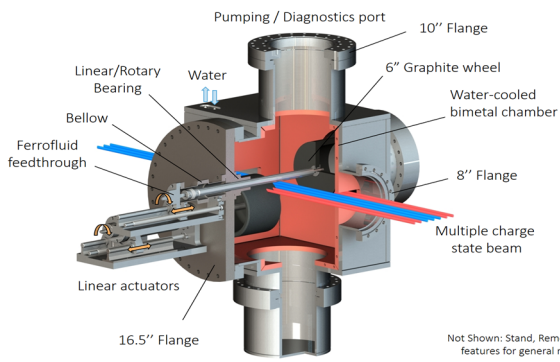

Figure 3: Intermediate-power charge selector design (1″ = 25.4 mm).

Collimation

The desired high beam power can be achieved with a low beam current (<1 mA) in the CW driver linac. Hence space charge effects are mostly negligible, except in the ion source and LEBT. However, collimation is nevertheless required for several reasons:

ISBN: 978-3-95450-253-0 ISSN: 2673-5571 doi:10.18429/JACoW-HB2023-THC1I2

- Filamentation of the phase space distribution occurs due to the inherent nonlinear fields in the ion source and the high space charge due to extraction of multi-component ion beams. Efficient beam halo collimation in the LEBT is therefore needed.
- Contaminants (unwanted ion species produced by the source with rigidity close to that of the primary ion species) must be blocked by collimators and vacuum chambers in the post-stripper chicane and in FS1.
- Charge stripping increases the emittance due to scattering and energy straggling. Collimation downstream of the stripper is needed to intercept particles scattered to large angles.
- Beam losses by gas stripping occur due to the elevated pressure around the charge selector region.

A series of collimators are designed to intercept contaminants, ions created due to charge-exchange reactions, and beam halo produced by emittance growth. Collimation will significantly reduce uncontrolled beam losses. The collimators will be properly shielded to avoid high residual radiation levels in the linac tunnel.

PHASED TARGETRY DEPLOYMENT

Relative to proton facilities (Fig. 1), heavy-ion facilities face more challenges due to higher power deposition density and higher radiation damage. FRIB targetry and ancillary systems are in phased deployment (Table 2). Although most challenges were understood at the time of the project baseline, additional complexities became clear during facility commissioning and early operation.

The targetry lacks the fast beam-diagnostic sensors used for the linac. To mitigate this drawback, upstream magnet power supplies are monitored by interlocking machine protection systems. Further beam diagnostics are provided with thermal sensors, imaging cameras, and intercepting plates. The collimator located 1.5 m upstream of the target is segmented for individual temperature reading. This collimator intercepts the beam halo and produces signals for alignment of the beam onto the target.

Table 2: Phased Targetry and Ancillary System Deployment

EPOCH	1	2	3	4	5	6
Beam power	10 kW	20 kW	50 kW	100 kW	200 kW	400 kW
Rotatable target, 1 slice	■	■	■			
Rotatable target, multi-slice				■	■	■
Post-target shield				■	■	■
Beam dump 6° slant (S-shape)	■	■				
Beam dump 6° slant (S-shape), better cooling			■			
Rotatable beam dump, 1-mm wall				■	■	
Rotatable beam dump, 0.5-mm wall						■
Medium power ladder wedge system with adjustable slits (hands-on)	■	■	■			
High power wedge system (remote handling)				■	■	■
PPS upgrade with fast ionization chambers	■	■	■	■	■	■

Target

The target is expected to absorb ~ 25% of the primary beam power. Single-slice rotating graphite targets [5] are planned for a primary beam power of up to 50 kW. Multi-slice targets with an improved heat exchanger will be used for full-power beam operations.

The single-slice target consists of a graphite disc, a copper heat exchanger, a ceramic hub, and an Inconel spindle with bearings (Fig. 4). Recently, a high-emissivity coating was applied to the heat exchanger interior to enhance radiative cooling efficiency for the disc. Improvements are also made to the bearings and lubricant.

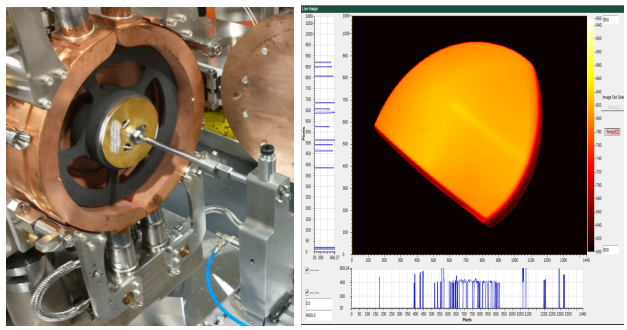

Figure 4: Left: single-slice graphite target inside the water-cooled copper enclosure. Right: thermal image of a 10 kW, 216.7 MeV/u ^{48}Ca beam on the target rotating at 500 revolutions per minute.

Beam Dump

The beam dump is designed to absorb ~ 75% of the primary beam power. Presently, a static dump is used with the beam incident at a 6° angle to reduce the deposited power density. An aluminum layer stops the primary beam from reaching the dump's cooling water channels to minimize activation of the water. The design is being improved to enhance the heat transfer by using several mini-channels for more effective water cooling (Fig. 5a). The ultimate beam dump (Fig. 5b) will be a rotating thin-wall water-filled drum, with the water flow serving both to cool the wall and stop the primary beam within the drum [9].

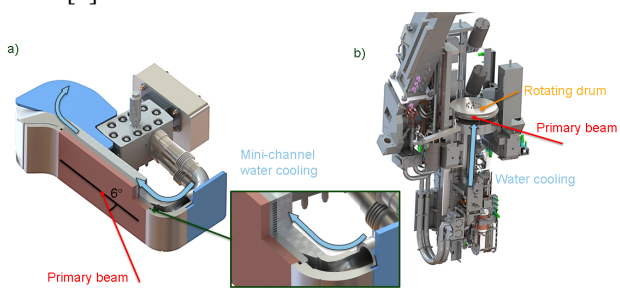

Figure 5: (a) Intermediate mini-channel beam dump and (b) rotating beam dump.

Wedge

A wedge intercepts secondary rare-isotope beams for improved isotope separation. The wedge has a unique shape to help maintain achromaticity at the downstream focal plan where undesired species are stopped at the slits. Wedge upgrades are planned, include the addition of remote handling capability and better tolerance to beam heating. A variable wedge system is being developed to increase tuning flexibility and operational availability.

Remote Handling

With up to 400 kW of beam on target, activation and radioactive waste generation make remote handling

ISBN: 978-3-95450-253-0 ISSN: 2673-5571 doi:10.18429/JACoW-HB2023-THC1I2

mandatory. Our remote handling design features combine hands-on and fully-remote operations to maximize efficiency and minimize operational costs. Presently, 4 hours after turn-off, the Target Hall can be accessed by trained personnel for hands-on work to prepare for subsequent fully-remote operations to handle highly-activated components.

Remote handling is routinely used for target disc and wedge changes during user operations and annual maintenance of the beam dump. Tooling and procedures are newly developed for changing the target bearing cartridge and applying the high-emissivity coating to the target heat exchanger (Fig. 6). Duplicate target and wedge assembly modules are being developed to allow quick reconfigurations (< 24 hour) during user experiments.

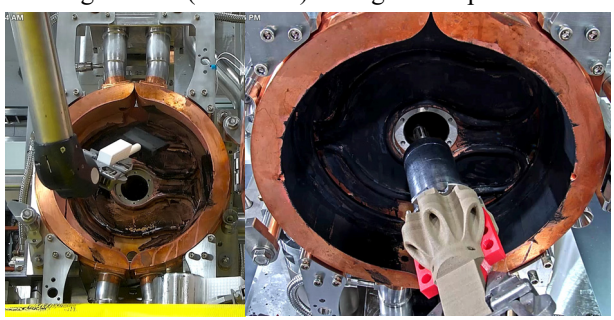

Figure 6: Target remote work: heat exchanger coating (left); bearing cartridge replacement (right).

BEAM LOSS BUDGET, RADIOLOGICAL CONTROL, PERSONNEL PROTECTION

Managing controlled beam loss and minimizing uncontrolled beam loss are crucial for maintaining radiologically sound operations with hands-on maintenance. The "loss budget" (Tables 3 – 5; MEBT: Medium Energy Beam Transport; LS: Linac Segment; F-Cup: Faraday Cup; RI: Rare Isotope) is the basis for shielding design, radiological impact control, personnel protection systems (PPS), environmental impact assessment and protection, and remote handling.

Personnel Protection

As FRIB is located in the middle of a university campus, the PPS response time must be fast to shut off beam in the worst-case incident scenarios to keep the integrated dose rate below the regulatory limit. Presently, we use commercial fast neutron monitors with a total system response time < 0.3 s, which allows for intermediate-power operation with the present shielding. As we increase the beam power, another PPS layer is being added for prompt radiation hazard mitigation: the "fast beam containment system" consists of ion chambers, beam inhibit devices to shut off the RFQ power, and connecting optical fiber. Among various failure modes (Table 6), the most demanding scenario corresponds to the primary beam being inadvertently delivered to the secondary beam line.

Table 3: Estimated Controlled Primary Beam Loss for Typical 400 kW Operation

Mechanism	Location	Power [kW]
Front end beam tuning	MEBT F-cup	0.1
$\beta = 0.041$ beam tuning	LS1 Nb plate	0.002
LS1 beam tuning	FS1a dump	0.015
LS1 beam tuning	FS1b dump	0.5
Charge stripping loss	FS1 stripper	1.3
Unwanted beam collection	FS1 selector	7-12
Unwanted charge state and ion contaminants collection	FS1 45° dipoles	0.1-0.4
Beam halo and ECR ion contaminants interception	Collimator 1-5	0.1-1.7
Charge exchange halo	Collimator 6-7	0.02
LS1 beam tuning	FS1 F-cup	0.03
LS2 beam tuning	FS2 dump	0.14
LS2 beam tuning	FS2 F-cup	0.03
Linac beam tuning	BDS dump	0.14
Targetry protection	Collimators	0.1
RI production	Target	< 80
Spent beam	Beam dump	< 320

Table 4: Estimated Controlled Secondary Beam Loss for Typical 400 kW Operation

Mechanism	Location	Power [kW]
Target scattering	Post-target shield	< 15
RI beam cleaning	Fragment catchers	< 20
Post-target scattering	Thermal armors	< 17
Post-target scattering	Collimators	< 9
RI beam	Wedge	< 2
RI beam cleaning	Wedge slits	< 3
RI beam cleaning	Separator slits	< 5
RI beam cleaning	Focal plane slits	< 2

Table 5: Estimated Uncontrolled Beam Losses for Typical 400 kW Operation

Mechanism	Location	Power
Stripper scattering	Downstream of stripper	<3 W/m at 17 MeV/u
Uncontrolled loss	All locations	< 1 W/m

Table 6: Accidental Beam Loss Scenarios for Typical 400 kW Operation (MPS: Machine Protection System)

Mechanism	Power	Response Time	
		MPS	PPS
Damaged stripper	Small fraction of 50 kW	35 µs	N/A
Damaged target	Large fraction of 400 kW	200 µs	7 ms

ISBN: 978-3-95450-253-0 ISSN: 2673-5571 doi:10.18429/JACoW-HB2023-THC1I2

Non-conventional Utilities

The non-conventional utilities (NCU) provide cooling for the targetry devices and handle transferred radioactivity accordingly. They include 2 closed cooling loops, centrifugal pumps, heat exchangers, gas-liquid separators, drain tanks, and instrumentation; auxiliary systems include a hydrogen recombiner, a clean-up system, and a low-level liquid waste system. The H recombiner was recently commissioned (Fig. 7); it is designed to catalytically recombine H_2 produced by water radiolysis with O_2 and capture gaseous radionuclides generated during operation. The clean-up system to remove particulate and ionic impurities from the cooling water is being upgraded for remote handling capability and easier maintenance.

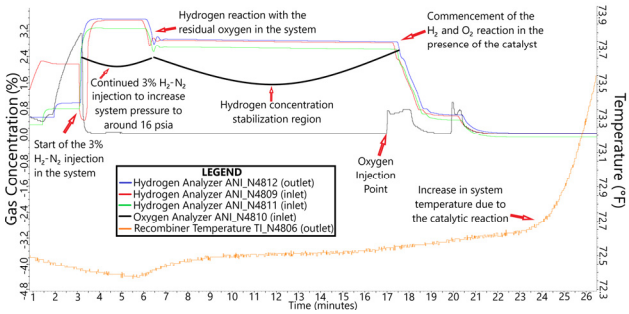

Figure 7: Concentration of H_2 and O_2 and temperature variation in the H recombiner during injection of 3% H_2-N_2 gas mixture with subsequent injection of pure O_2.

LEGACY SYSTEM RENOVATION

Cryogenics

The FRIB central helium refrigeration system commissioned in 2018 presently supports operation of the cryomodules in the driver linac and SC magnets in the linac, Target Hall and pre-separator area [10]. The remaining experimental areas are supported by the legacy National Superconducting Cyclotron Laboratory (NSCL) cryogenic He refrigeration system originally designed in the mid 1970's, refurbished in 2000, and reconfigured for FRIB [11]. Although this solution protects the FRIB central system from frequent configuration changes and contamination risks, the NSCL system must be upgraded for stability, reliability, efficiency, and support of future expansion. The cryogenic infrastructure prioritizes:

- Efficient operation to minimize the cost of utilities (electricity and liquid nitrogen), with the patented floating pressure process cycle [12], adjusting the cryoplant cycle to the loads;
- Maximum availability with adequate redundancies;
- Phased commissioning for evolving configurations, matching user needs with minimal down-time;
- Multiple independent sub-systems for maintainability, with expandability;
- Automated operation with a minimal work force.

The upgrade include the addition of a 4.5 K cold box, a shield cold box, and a shield cold box compressor.

Recovery, purification, and preservation of the helium inventory is of critical importance. The total liquid He inventory at FRIB is ~ 40 000 liters. A high capacity (~ 30 g/s) He recovery compressor and a helium purifier are being developed for improved He preservation. A high-pressure (200 bar) He storage system is also planned to manage the He inventory during operational transients. These systems will allow for recovery of the entire FRIB He inventory. The storage system will be able to accommodate a year's time frame of He inventory onsite and will provide long-term storage, minimizing the operational impact of fluctuations in the He supply chain.

Magnets

Legacy NSCL SC magnets make up ~ 50% of the total number of SC magnets at FRIB; they are mainly in beam lines to experimental stations. The magnets have been in service for > 20 years and present known challenges, including (i) insulating vacuum issues; (ii) flawed design features that are susceptible to introducing He leaks; and (ii) limitations in performance due to outdated magnet technology. We are currently refurbishing spare magnets to mitigate these issues. This includes replacing the vapor-cooled current lead piping and adjusting the pressure relief configurations. The refurbishment program is phased to minimize risks [13]. Simultaneously, we are developing new magnet technology using high temperature superconductors (HTS), innovative iron-free coil designs, and advanced conduction cooling. The ultimate objective is to replace all of the legacy magnets with new designs to significantly enhance operational performance.

Controls

The FRIB scope was limited to the exit of the fragment separator that supplies the NSCL secondary beam lines. The control system for the secondary beam lines must be upgraded to the standard of the FRIB control system to improve network security and maintainability. A 3-phase upgrade is planned: (1) disconnect the system from the NSCL network and connect it to the new secure FRIB control network; (2) replace obsolete control devices to mitigate network security risks and improve maintainability; (3) replace control devices with standardized FRIB devices for efficient maintenance and reduced spare inventory. Phases 1 and 2 are mostly complete, while Phase 3 is ongoing.

AUTOMATION AND MACHINE LEARNING

Automation is important both for high-availability operation and the power ramp-up. For a facility consisting of hundreds of beam line devices, efficient operation is only possible through automation. Moreover, automation can reduce human error, reduce training efforts, and improve operational consistency; for tasks that require a faster reaction time than humanly possible, e.g. quickly recovering a room temperature cavity from a trip, automation is the only solution [14]. Machine learning (ML) may facilitate challenging tasks for efficient high-power operation.

ISBN: 978-3-95450-253-0 ISSN: 2673-5571 doi:10.18429/JACoW-HB2023-THC1I2

Front End Automation

Automatic turn-on (cold start) and fast trip recovery have been implemented for room temperature cavities. In particular, the RFQ, which is frequency-controlled by temperature, must be restarted within a few seconds after a cavity trip to avoid lengthy down time. R&D efforts using ML have been initiated to further optimize frequency control of the RFQ to reduce the turn-on time.

Linac Automation

Linac automation is being implemented at both the device level and the system level. At the device level, turn-on/turn-off for a cavity or solenoid is programmed in the input-output controller (IOC) using state notation language (SNL). At the system level, a few buttons on the graphical user interface (GUI) may be used for auto-on/off commands to devices throughout the linac, executed at the device level. This is usually implemented with Python scripts, which provide great flexibility. Python scripts are also used for prototyping device-level tasks at the early stages when frequent and quick iterations are necessary.

Linac automation is particularly helpful for the FRIB single event effects (FSEE) user program [15], as the users need to access the experimental area in the linac tunnel frequently (sometimes more than once per hour). All SRF cavities are turned off for each tunnel access. With on/off automation, the cavities can be turned off in a few seconds and turned on in < 2 minutes (Fig. 8).

Other tasks related to linac operation that have been automated include field "reduce and recover" for cavities with high field emission; pneumatic tuner valve calibration for half wave resonators (HWRs); conditioning of cavity multipacting; magnet degaussing; and linac emergency shutdown [16].

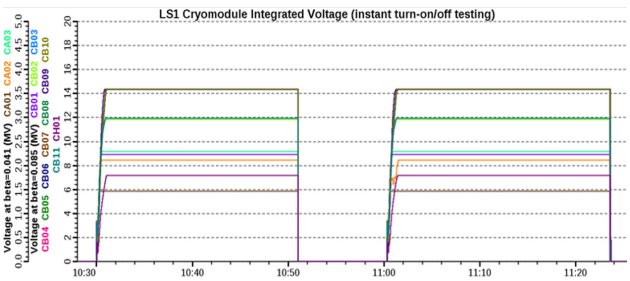

Figure 8: Fast turn-on/turn-off of LS1 SRF cavities.

Artificial Intelligence and Machine Learning

Machine learning may become an essential tool for boosting FRIB beam power and ensuring safe operation. Leveraging real-time and archived operational data, ML techniques create data-driven models, which may be useful for faster beam tuning, improved control of beam losses, fast anomaly detection, and designing advanced controls for accelerator hardware.

ML has been used for accelerators to construct surrogate models that encapsulate the highly non-linear, and high-dimensional dynamics of beams and accelerator components. ML is particularly valuable when conventional physics-based models are either absent or excessively intensive in computation time. ML has already been applied to the FRIB front end, demonstrating faster tuning optimization [17]. Tomography techniques for reconstructing the beam distribution have been studied and experimental trials are planned [18].

SUMMARY

The Facility for Rare Isotope Beams has been operating for more than a year, delivering beams for both scientific and industrial experiments with the desired reliability and availability. The primary beam power is being steadily raised from 1 to 10 kW. To ramp up to the ultimate design beam power of 400 kW, efforts are focused on phased linac improvements, phased targetry system deployments, control of beam loss, radiological impacts, legacy system renovation, automation, and machine learning. The power ramp-up campaign and the proposed FRIB upgrade to double the primary-beam energy to 400 MeV/nucleon [19] will significantly enhance FRIB's discovery potential.

ACKNOWLEDGMENTS

FRIB accelerator systems design and construction have been facilitated under work-for-others agreements with many DOE-SC national laboratories including ANL, BNL, FNAL, JLab, LANL, LBNL, ORNL, and SLAC, and in collaboration with institutes worldwide including BINP, KEK, IHEP, IMP, INFN, INR, RIKEN, TRIUMF, and Tsinghua University. The cryogenics system was developed in collaboration with the JLab cryogenics team. The SRF development benefited greatly from the expertise of the low-β SRF community. FRIB has been collaborating with ANL on RF coupler and tuner developments, assisted by JLab for cryomodule design, and by FNAL and JLab on cavity treatments.

We thank the FRIB Accelerator Systems Advisory Committee for their valuable guidance and colleagues who participated in FRIB accelerator peer reviews, including G. Ambrosio, J. Anderson, J. Aoki, D. Arenius, C. Barbier, W. Barletta, G. Bauer, G. Biallas, J. Bisognano, W. Blokland, S. Bousson, P. Brindza, M. Calviani, S. Caspi, M. Champion, D. Cossairt, M. Crofford, C. Cullen, D. Curry, R. Cutler, M. Dayton, G. Decker, J. Delayen, J. Delong, G. Dodson, J. Donald, H. Edwards, J. Error, I. Evans, M. Fitton, J. Fuerst, Y. Iwamoto, T. Khabiboulline, F. Kornegay, K. Kurukawa, J. Galambos, J. Galayda, G. Gassner, P. Ghoshal, J. Gilpatrick, C. Ginsburg, A. Gottberg, S. Gourlay, J. Haines, M. Harrison, S. Hartman, S. Henderson, G. Hoffstaetter, J. Hogan, S. Holmes, M. Howell, P. Hurh, R. Kersevan, A. Hodgkinson, N. Holtkamp, H. Horiike, K. Hosoyama, C. Hovater, H. Imao, R. Janssens, R. Keller, J. Kelley, M. Kelly, P. Kelley, J. Kerby, S. H. Kim, A. Klebaner, J. Knobloch, R. Lambiase, M. Lamm, Y. Li, C. LoCocq, C. Luongo, K. Mahoney, S. Maloy, J. Mammosser, T. Mann, A. P. Marcone, R. May, S. Meigo, W. Meng, N. Mokhov, D. Montierth, G. Murdoch, J. Nolen, W. Norum, H. Okuno, S. Ozaki, R. Pardo, S. Peggs, C. Peters, R. Petkus, C. Pearson, F. Pellemoine,

ISBN: 978-3-95450-253-0 ISSN: 2673-5571 doi:10.18429/JACoW-HB2023-THC1I2

T. Peterson, C. Piller, J. Power, T. Powers, J. Preble, J. Price, D. Raparia, J. Rathke, A. Ratti, T. Roser, M. Ross, R. Ruland, J. Sandberg, R. Schmidt, W. J. Schneider, D. Schrage, P. Schuh, D. Senor, S. Sharma, I. Silverman, K. Smith, J. Sondericker, W. Soyars, C. Spencer, R. Stanek, M. Stettler, W. C. Stone, J. Stovall, H. Strong, L. T. Sun, Y. Than, J. Thomason, J. Theilacker, Y. Tian, M. Thuot, J. Tuozzolo, V. Verzilov, R. Vondrasek, P. Wanderer, K. White, D. Winder, M. Wiseman, W. Wohlmuther, P. Wright, H. Xu, K. Yoshida, L. Young, and A. Zaltsman; and colleagues who advised and collaborated with the FRIB team including A. Burrill, A. C. Crawford, K. Davis, X. Guan, P. He, Y. He, A. Hutton, P. Kneisel, R. Ma, K. Macha, G. Maler, E. A. McEwen, S. Prestemon, J. Qiang, T. Reilly, W. Sommer, R. Talman, J. Vincent, X. W. Wang, J. Xia, Q. Z. Xing, and H. H. Zhang.

The FRIB accelerator design is executed by a dedicated team in the FRIB Accelerator Systems Division in close collaboration with the Science Division headed by B. Sherrill, the Experimental Systems Division headed by G. Bollen, the Conventional Facility and Infrastructure Division, and the Chief Engineer's team headed by D. Stout, with support from the FRIB project controls, procurement, and ES&H teams. We thank our industrial partners in the USA and worldwide for their support to FRIB for design, R&D, construction, commissioning, and operations.

REFERENCES

[1] J. Wei *et al.*, "Accelerator commissioning and rare isotope identification at the Facility for Rare Isotope Beams", *Mod. Phys Lett. A,* vol. 37, p. 2230006, 2022. doi:10.1142/S0217732322300063

[2] P. N. Ostroumov *et al.*, "First simultaneous acceleration of multiple charge states of heavy ion beams in a large-scale superconducting linear accelerator", *Phys. Rev. Lett.,* vol. 126, p. 114801, 2021. doi:10.1103/PhysRevLett.126.114801

[3] T. Kanemura *et al.*, "Experimental demonstration of the thin-film liquid-metal jet as a charge stripper", *Phys. Rev. Lett.,* vol. 128, p. 212301, 2022. doi:10.1103/PhysRevLett.128.212301

[4] H. Ren *et al.,* "Development and status of the FRIB 28 GHz SC ECRIS", *J. Phys.: Conf. Ser.,* vol. 2244, p. 012008, 2022. doi:10.1088/1742-6596/2244/1/012008

[5] F. Pellemoine *et al.,* "Thermo-mechanical behaviour of a single slice test device for the FRIB high power target", *Nucl. Instrum. Methods Phys. Res., Sect. A*, vol. 655, pp 3-9, 2011. doi:10.1016/j.nima.2011.06.010

[6] T. Xu *et al.*, "Completion of FRIB superconducting linac and phased beam commissioning", in *Proc. SRF'21*, East Lansing, MI, USA, Jun.-Jul. 2021, pp. 197-202. doi:10.18429/JACoW-SRF2021-MOOFAV10

[7] J. Guo *et al*., "FRIB ECR ion sources operation and future development" presented at ICIS'23, Victoria, Canada, Sep. 2023, Paper 131, unpublished.

[8] T. Shen *et al.*, "Design and development of a 28 GHz Nb3Sn ECR ion source superconducting magnet", submitted to *IEEE Trans. Appl. Supercond.*

[9] M. Avilov *et al.*, "Thermal, mechanical and fluid flow aspects of the high power beam dump for FRIB", *Nucl. Instrum. Methods Phys. Res., Sect. B,* vol. 376, pp 24-27, 2016. doi:10.1016/j.nimb.2016.02.068

[10] P. Knudsen *et al*., "FRIB helium refrigeration system commissioning and performance test results", *IOP Conf. Ser.: Mater. Sci. Eng.*, vol. 755, p. 012090, 2020. doi:10.1088/1757-899X/755/1/012090

[11] N. Hasan *et al*., "Design, Fabrication and Installation of the cryogenic distribution system for re-configured FRIB A1900 fragment separator", in *Proc. ICEC28-ICMC 2022*, Hangzhou, China, Apr. 2022.

[12] V. Ganni and P. Knudsen; "Optimal design and operation of helium refrigeration systems using the Ganni Cycle". *AIP Conf. Proc.*, vol. 1218, pp.1057-1071, 2010. doi:10.1063/1.3422267

[13] Y. Choi *et al*., "Overview of fragment separator superconducting magnets in the Facility for Rare Isotope Beams", *IEEE Trans. Appl. Supercond.,* vol. 33, no. 5, p. 4100305, 2023. doi:10.1109/TASC.2023.3244141

[14] S. Zhao *et al*., "Automation of RF and cryomodule operation at FRIB", in *Proc. HIAT'22*, Darmstadt, Germany, Jun.-Jul. 2022, pp. 136-139. doi:10.18429/JACoW-HIAT2022-TH1C3

[15] S. Lidia *et al*., "A Heavy-Ion single-event effects test facility at Michigan State University", *2022 IEEE Radiation Effects Data Workshop (REDW) (in conjunction with 2022 NSREC)*, Provo, UT, USA, Jul. 2022, pp. 1-7. doi:10.1109/REDW56037.2022.9921718

[16] W. Chang *et al.,* "Automation of FRIB SRF cavities and SC solenoid turn-on/off", presented at SRF'23, Grand Rapids, MI, USA, Jun. 2023, paper FRIBA05, in press.

[17] P. Ostroumov *et al*., "FRIB from commissioning to operation", presented at HB'23, Geneva, Switzerland, Oct. 2023, paper MOA1I2, these proceedings.

[18] A. D. Tran and Y. Hao, "Beam tomography with coupling using maximum entropy technique", in *Proc. IPAC'23*, Venice, Italy, May 2023, pp. 3944-3947. doi:10.18429/JACoW-IPAC2023-THOGB2

[19] A. Gade *et al.* Eds., "FRIB400: The scientific case for the 400 MeV/u energy upgrade of FRIB," FRIB, Michigan State University, East Lansing, MI, USA, June 2019, updated Feb. 2023. https://frib.msu.edu/_files/pdfs/frib400_final.pdf